Electro-Fenton treatment of the analgesic tramadol: Kinetics, mechanism and energetic evaluation

Hélène Monteil, Nihal Oturan, Yoan Péchaud, Mehmet Oturan

Electro-Fenton treatment of the analgesic tramadol: kinetics, mechanism and energetic evaluation

Hélène Monteil, Nihal Oturan, Yoan Péchaud, Mehmet A. Oturan*

Université Paris-Est, Laboratoire Géomatériaux et Environnement (EA 4508), UPEM, 5 Bd Descartes, 77454 Marne-la-Vallée, Cedex 2, France.

* Corresponding author: Mehmet.Oturan@univ-paris-est.fr

Abstract

The removal of the analgesic tramadol (TMD) from water was studied by electro-Fenton (EF) process using BDD anode. Hydroxyl radicals (•OH) generated in this process are very strong oxidants and able to successfully oxidize TMD until its total mineralization in aqueous solution. The oxidative degradation of TMD was very rapid with complete disappearance of 0.1 mM (26.3 mg L^{-1}) TMD in 10 min at 500 mA constant current electrolysis. The absolute (second order) rate constant for oxidation of TMD by •OH was determined using competition kinetic method and found to be (5.59 ± 0.03) × 10^9 M^{-1} s^{-1}. The quasi-complete mineralization of the 0.1 mM TMD solution was obtained in 6 h electrolysis at 500 mA current. Several oxidation reaction intermediates were identified using GC-MS analysis. Oxalic, glyoxylic and fumaric acids were identified and their evolution during electrolysis was followed along treatment. Ammonium and nitrate ions, released during the treatment, were also considered. Based on these data and TOC removal results, a possible mineralization pathway was proposed.

Keywords: Tramadol; Electro-Fenton; Advanced oxidation; Wastewater treatment; Mineralization; Energy consumption

1. Introduction

Residual pharmaceuticals in wastewaters have become a hot topic nowadays. The consumption of pharmaceuticals have increased in the last twenty years because of population growth, population ageing and the decrease of their price (Daughton 2003). This increasing consumption has resulted in more and more residual pharmaceuticals in natural water body especially because the wastewater treatment plants (WWTPs) were not designed to eliminate them properly (Kim et al. 2009; Verlicchi et al. 2013). Once in the environment, the pharmaceuticals are responsible for aquatic toxicity, resistance development in bacteria, genotoxicity and endocrine disruption (Loos et al., 2013; Antonopoulou and Konstantinou, 2016). Among pharmaceuticals, analgesics and anti-inflammatories are very often prescribed as they are general treatments to fight against pains. The tramadol (TMD) is a centrally acting analgesic used in case of moderate to severe pain (Ghalwa et al., 2014; Antonopoulou and Konstantinou, 2016). This medicine is widely used, for instance, around 24 tons of TMD was prescribed in Germany in 2012 (Lütke Eversloh et al. 2015). On the other hand, it is not efficiently removed by WWTPs as it was detected in effluents from households and hospitals after treatment as well as in surface waters (Hummel et al., 2006; Rúa-Gómez and Püttmann, 2012, 2013). TMD was also identified as one of the 12 pharmaceuticals and personal care products the most detected in the Yeongsan river in Korea with concentrations upper than 200 ng L^{-1} (Park et al. 2018). For all these reasons, it is important to eliminate this pharmaceutical from the environment. Therefore, its removal from water requires the use of non-conventional techniques such as advanced oxidation processes (Oturan and Aaron 2014). TMD was successfully degraded by heterogeneous photocatalysis with TiO_2 (Antonopoulou and Konstantinou, 2016; Lambropoulou et al., 2017), ferrate and O_3 (Zimmermann et al. 2012)

and potential and current controlled electrolysis (Ghalwa et al. 2014; Lütke Eversloh et al. 2015). The literature survey on the degradation of TRM using advanced oxidation processes is summarized in Table SM-1, showing low efficiency of the processes tested.

On the other hand, the electrochemical AOPs (EAOPs) proved great efficiency in destruction of persistent organic pollutants (Brillas et al. 2009; Sirés and Brillas 2012; Rodrigo et al. 2014; Monteil et al. 2018; Nidheesh et al. 2018). Electro-Fenton (EF) process is among of the most popular EAOPs and has not yet been applied to treatment of TMD. It is based on the electrocatalytic generation of the Fenton's reagent from Eqs. 1 and 2, using compressed air and externally added catalyst (Fe^{2+} ion at low concentration), respectively. Then, $^{\bullet}OH$ generated through electrochemically promoted Fenton reaction (Eq. 3) oxidize/mineralize organic pollutants (Oturan 2000; Brillas et al. 2009; Zhou et al. 2018).

$$O_2 + 2H^+ + 2e^- \rightarrow H_2O_2 \quad (1)$$

$$Fe^{3+} + e^- \rightarrow Fe^{2+} \quad (2)$$

$$Fe^{2+} + H_2O_2 \rightarrow Fe^{3+} + {}^{\bullet}OH + OH^- \quad (3)$$

The nature of electrode material used in this process is very important. Having a large O_2 reduction overpotential, carbonaceous cathodes promote the formation of H_2O_2 while avoiding the 4-electron reduction of O_2 (Eq. 4) (Sirés et al. 2007; Pimentel et al. 2008). In the same way, the use of a high O_2 overpotential electrode such as BDD promotes the formation of high amount of $^{\bullet}OH$ physically adsorbed on anode (M) surface, M($^{\bullet}OH$), according to the Eq. 5 (Panizza and Cerisola, 2009; Rodrigo et al., 2010; Nidheesh et al., 2019).

$$O_2 + 4H^+ + 4e^- \rightarrow 2H_2O \quad (4)$$

$$M + H_2O \rightarrow M({}^{\bullet}OH) + H^+ + e^- \quad (5)$$

This paper is focused on the efficient oxidation and mineralization of TMD solutions using electro-Fenton process with BDD anode. The kinetics of oxidative degradation and

77 mineralization of TMD solutions were extensively investigated under the best operating
78 conditions of catalyst concentration and current applied. The reaction intermediates formed
79 during the oxidation process, the short-chain carboxylic acids as final by-products before
80 complete mineralization and mineral end-products were identified to propose a plausible
81 mineralization pathway.
82

83 2. Materials and methods

84 2.1 Chemicals

85 The analgesic TMD ($C_{16}H_{25}NO_2$) was supplied by Sigma Aldrich. Iron (II) sulfate
86 heptahydrate in analytical grade (catalyst source, 99% purity) came from Acros Organics.
87 Na_2SO_4, K_2SO_4 used as supporting electrolyte were purchased from Merck and Acros,
88 respectively. Oxalic, fumaric and glyoxylic acids were obtained from Acros and Fluka.
89 Ultrapure water obtained from a Millipore Milli-Q Simplicity 185 system with resistivity >18
90 MΩ cm at 25 °C was used to prepare the solutions. Analytical grade H_2SO_4 and NaOH were
91 provided by Acros and used to set solution pH.

92 2.2. Electrochemical equipment

93 A 7 cm diameter cylindrical glass of 250 mL at room temperature was used as
94 electrochemical cell to perform the experiments. The cell was equipped with a 3D carbon felt
95 (18.0 cm × 5.0 cm × 0.5 cm, from Mersen, France) as cathode and a 25-cm^2 BDD film on
96 niobium support (CONDIAS GmbH, Germany) as cathode (A schematic representation of the
97 electrochemical cell used in this work can be found in references: Brillas et al., 2009 and
98 Ganiyu et al., 2019) . The carbon felt was placed on the inner wall of the cell covering the
99 total internal perimeter. The electrochemical cell was powered by a Hameg HM8040 triple
100 power DC supply. To ensure a good mixing of the solution a magnetic PTFE bar and air

bubbling were used; the bubbling was started 5 min before the beginning of the experiment to have the solution saturation in O_2 to promote H_2O_2 generation at an optimal rate (in function of the current applied). To regulate the pH to the optimal value of 3.0 for EF process (Kremer, 2003; Brillas et al., 2009) a CyberScan pH 1500 pH meter (Eutech Instruments) was used.

2.3 Analytical procedures

The TMD concentration decay was followed by HPLC using a Merck Lachrom Liquid chromatography system by injecting 20 µL samples into a reverse phase column, Purospher RP-18, 5 µm, 25 cm × 4.6 mm (i.d.), at 40 °C and coupled with a DAD detector. The mobile phase was a mixture of methanol / phosphate buffer 40:60 (v/v) at a flow rate of 0.6 mL min^{-1}. The detection was carried out at 228 nm. The phosphate buffer was composed of 3.5 g of potassium phosphate monobasic and 17.8 g of dipotassium hydrogen phosphate in 1 L of ultra-pure water and the pH was adjusted to 6.0 using orthophosphoric acid.

To quantify the generated carboxylic acids the same HPLC system was used equipped with a Biorad column (9 µm, 250 mm × 4.6 mm) and the DAD detector set to 220 nm. The mobile phase was a 4 mM solution of sulfuric acid at 0.6 mL min^{-1}. Calibration curves were prepared using standard solutions.

Ionic chromatography analyses were performed by injecting 25 µL samples into a Dionex ICS-1000. Nitrate and nitrite concentrations were measured with an Ion Pac AS4A-SC, 25 cm× 4 mm (i.d.), anion-exchange column, linked to an IonPac AG4A-SC, 5 cm × 4 mm (i.d.), column guard at 35°C. The mobile phase was a mixture of 1.7 mM sodium bicarbonate ($NaHCO_3$) and 1.8 mM sodium carbonate (Na_2CO_3) at a flow rate of 1 mL min^{-1}. To improve the sensitivity of the detector, an ASRS-ULTRA II self-regenerating suppressor was used. Ammonium concentration was measured with an IonPac CS12A, 25 cm × 4 mm (i.d.), cation-

125 exchange column, linked to an IonPac CG12A, 5 cm × 4 mm (i.d.) guard column at 30°C. A
126 CRS-ULTRA II suppressor was also used. The mobile phase was a solution of 9.0 mM
127 sulfuric acid at a flow rate of 1.0 mL min^{-1}.

128 Total organic carbon (TOC) was measured before starting the treatment and at different
129 treatment times to evaluate the mineralization degree of the solution under study with a
130 Shimadzu VCSH TOC analyzer according to the 680 °C catalytic combustion method using
131 platinum as catalyst. The calibration was performed with a potassium hydrogen phthalate
132 solution. Reproducible TOC values with ± 2% accuracy were found using the non-purgeable
133 organic carbon method by injecting 50 µL.

134 The mineralization current efficiency (MCE%) for each treated solution at given electrolysis
135 time t (h) was calculated from TOC values, according to the Eq. 6.

136 $$MCE(\%) = \frac{n\,F\,V\,(TOC(0)-TOC(t))}{4.32 * 10^{7} m\,I\,t} * 100 \quad (6)$$

137 where TOC(0) –TOC(t) is the TOC decay (mg carbon L^{-1}), m is the number of carbon atoms
138 of the TMD (16), *I* is the current applied (A), *V* is the volume of the solution (L), 4.32 × 10^7
139 is a conversion factor to homogenize units. The value n was taken as 82 considering that each
140 TMD molecule is mineralized into CO_2 and ammonium (Eq. 7). The concentration of nitrates
141 was much lower than that of the ammonium ions, thus the nitrate were not considered in the
142 mineralization equation (Monteil et al. 2019).

143 $$C_{16}H_{25}NO_2 + 30H_2O \rightarrow 16CO_2 + 81H^+ + NH_4^+ + 82e^- \quad (7)$$

144 The energy consumed in kWh per g TOC removed was given by Eq. 8 (Brillas et al. 2009).

145 $$EC\left(\frac{kWh}{gTOC}\right) = \frac{E_{cell} * I * t}{(TOC(0)-TOC(t)) * V} \quad (8)$$

146 To identify the intermediates formed during TMD mineralization, 1 mM TMD solution was
147 electrolyzed at 500 mA during 8 min. Direct extraction of resulting organics with ethyl acetate

was performed, then this solution was completely evaporated under vacuum and diluted again in a few µL. 3 µL of this solution were then injected into a TG-5Ms 0.25 mm, 30 m, 0.25 mm (i.d.), column of a Thermo Scientific devise equipped with a TRACE 1300 gas chromatography coupled to an ISQ single quadrupole mass spectrophotometer operating in electron ionization mode at 70 eV. The temperature ramp for this column was 100 °C during 1 min, 20 °C min^{-1} to 280 °C and kept at this temperature for 15 min. The temperature of the inlet and detector were 200 and 250°C, respectively. The mobile phase was composed of Helium gas at a flow rate of 1.5 mL min^{-1}.

When error bars are given on the graphs, they are calculated based on the standard deviation of the different experiments.

3. Results and discussion

3.1 Degradation kinetics of TMD

The determination of the degradation rate of pollutants during the treatment constitutes an appropriate way to measure the efficiency of a process. In EF process, the degradation of organic pollutants is occurring thanks to the simultaneous generation of homogeneous (•OH) and heterogeneous M(•OH) hydroxyl radicals formed in the bulk solution through Fenton reaction (Eq. 3) and on the surface of the anode (Eq. 4), respectively (Özcan et al., 2008; Sirés et al., 2014). Among the operating parameter, the most influential are the solution pH, the current applied and the catalyst nature and concentration. Concerning the solution pH, it is now well-established as pH near 3, but the value of current and catalyst concentration needs preliminary trials to determine optimal conditions (Brillas et al. 2009; Dominguez et al. 2018; Monteil et al. 2018).

171 Among different catalysts, iron ions (Fe^{2+} or Fe^{3+}) constitute the best choice (Pimentel et al.,
172 2008; Brillas et al., 2009; Oturan et al., 2010). Figure 1 depicts the degradation kinetics of
173 TMD for different Fe^{2+} concentrations between 0.05 and 0.5 mM under 100 mA constant
174 current. TMD is quickly degraded for the concentrations of 0.1 and 0.2 mM with complete
175 degradation reached at 10 min. Higher catalyst concentrations such as 0.5 mM lead to a
176 significant decrease in oxidation kinetics of TMD due to the enhancement of the wasting of
177 $^{\bullet}OH$ by Fe^{2+} (Eq. 9). Following the value of the apparent rate constants determined by
178 assuming pseudo-first order reaction kinetics (insert panels of Fig. 1), the concentration of 0.2
179 mM Fe^{2+} (corresponding to apparent rate constant of 0.47 min^{-1}) was found as the best value
180 for degradation of TMD by electro-Fenton process (Panizza and Cerisola, 2001; Dominguez
181 et al., 2018).

182 $$Fe^{2+} + {}^{\bullet}OH \rightarrow Fe^{3+} + OH^{-} \quad (9)$$

183 To clarify the effect of current on degradation kinetics of TMD, 0.1 mM TMD solution was
184 degraded under different currents (Fig. 2). As can be seen from Fig. 2, degradation rate of
185 TMD increases with rising the current from 50 to 500 mA. The complete disappearance of 0.1
186 mM TMD was achieved in 8, 10, 12 and 25 min for 500, 300, 100 and 50 mA, respectively.
187 This higher efficiency with high currents is linked to the enhancement of the rate of
188 electrochemical reactions (Eqs. 1 and 2) allowing the generation of high amount of $^{\bullet}OH$ in the
189 solution and M($^{\bullet}OH$) (Eq. 5) on the anode surface (Brillas et al. 2009). Therefore the value of
190 the rate constants increases from 0.21 min^{-1} for 50 mA to 0.70 min^{-1} for 500 mA.

191 However, the proportionality between the increase of the current and the apparent rate
192 constant is only followed for the two first current values. For instance, the degradation
193 kinetics curves corresponding to 300 and 500 mA are quite closed indicating that the effect of
194 increase in current is counterbalanced by the enhancement of the rate of side reactions. The
195 most important of these side reactions are: i) the H_2 evolution reaction (Eq. 10) which

competes with the production of H_2O_2 and ii) the O_2 evolution reaction in the bulk (Eq. 11) and on the anode (Eq. 12) which slow down the oxidation rate of TMD (Brillas et al., 2009; Sirés et al., 2014; Oturan and Oturan, 2018).

$$2\ H^+ + 2\ e^- \rightarrow H_2 \quad (10)$$

$$2\ H_2O \rightarrow O_2 + 4\ H^+ + 4\ e^- \quad (11)$$

$$2\ M(^{\bullet}OH) \rightarrow 2\ M + O_2 + 2\ H^+ + 2\ e^- \quad (12)$$

Figure SM-2 aims at testing the oxidation ability of the EF process for a range of initial concentrations of TMD between 0.1 and 0.5 mM. As expected, a quicker degradation occurred for the lowest concentration of 0.1 mM due to the low number of molecule to be oxidized. The time required for complete oxidation of TMD was around 20, 90, 150 and 180 min for 0.1, 0.2, 0.3 and 0.5 mM, respectively, under 500 mA constant current.

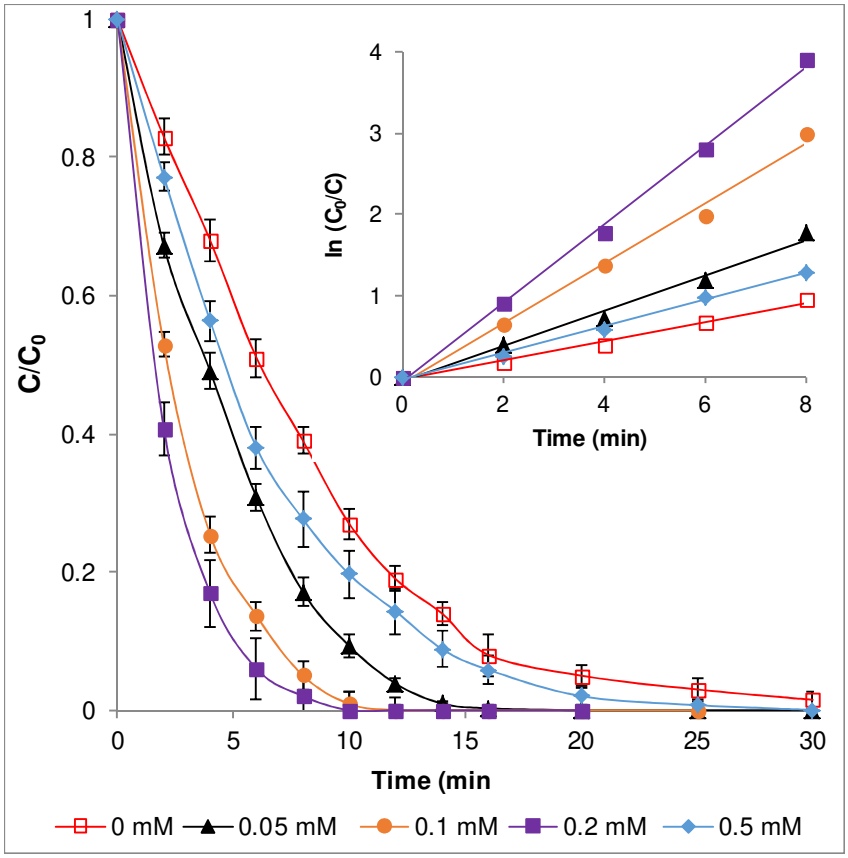

Fig. 1: Effect of catalyst (Fe^{2+}) concentration on the TMD decay kinetics at 100 mA constant current. $[TMD]_0$ = 0.1 mM, $[Na_2SO_4]_0$ = 0.05 M. The inset represents the kinetic analysis assuming pseudo-first order reaction kinetics for oxidation of TMD by hydroxyl radicals. a: y = 0.47x, R^2 = 0.997, b: y = 0.36x, R^2 = 0.990, c: y = 0.21x, R^2 = 0.984 and d: y = 0.16x, R^2 = 0.992.

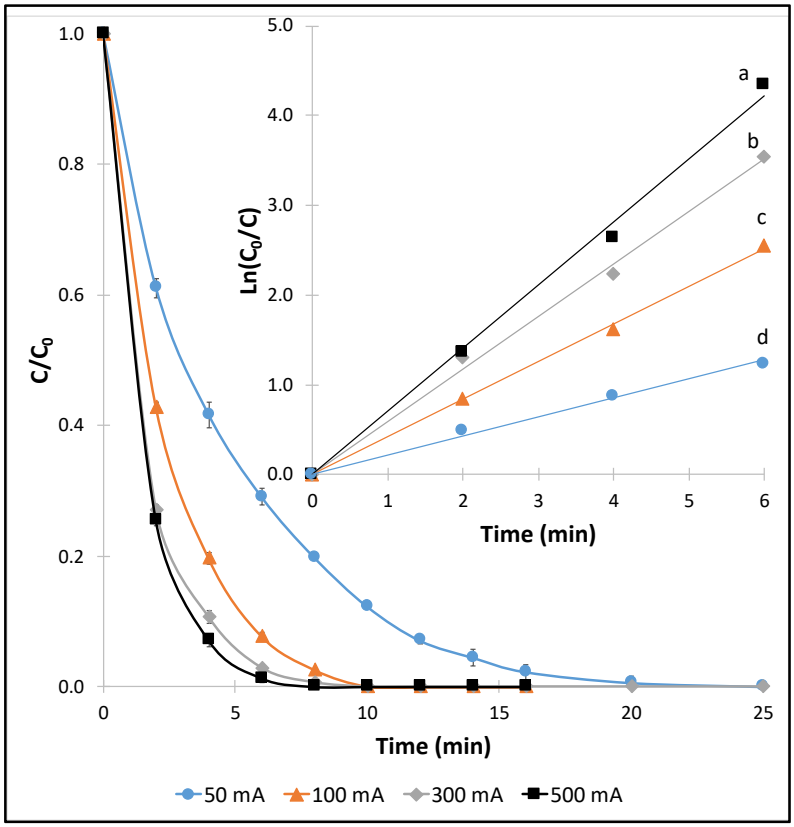

Fig. 2: Effect of current on degradation kinetics of 0.1 mM TMD in 0.05 M of Na_2SO_4 solution containing 0.2 mM Fe^{2+} (catalyst). The inset represents the kinetic analysis assuming pseudo-first reaction kinetics for oxidation of TMD by hydroxyl radicals. a: y = 0.7x, R^2 = 0.995, b: y = 0.59x, R^2 = 0.995, c: y = 0.42x, R^2 = 0.998 and d: y = 0.21x, R^2 =0.991.

The absolute rate constant for oxidation of TMD by •OH/M(•OH) was then evaluated using competition kinetics method (Oturan et al., 2010; Oturan and Aaron, 2014; Sopaj et al., 2016). This method is based on the competitive degradation of the molecule under study and a standard competitor for which the rate constant is well-known. Therefore, benzoic acid (BA)

with k_{BA} of 4.3×10^9 M^{-1} s^{-1} (Buxton et al. 1988) was selected as standard competitor. The determination of the absolute rate constant k_{TMD} is done according to the Eq. 13.

$$\ln\left(\frac{[TMD]_0}{[TMD]}\right) = \frac{k_{TMD}}{k_{BA}} \times \ln\left(\frac{[BA]_0}{[BA]}\right) \quad (13)$$

with k_{TMD} and k_{BA} the absolute rate constant for oxidation reaction of TMD and BA, respectively, by hydroxyl radicals. Degradation kinetics was carried out at 50 mA current to avoid the interference of the oxidation products. Using this equation, k_{TMD} was then calculated from the slop of the straight line of the Fig. 3 and found to be $(5.60 \pm 0.02) \times 10^9$ M^{-1} s^{-}.

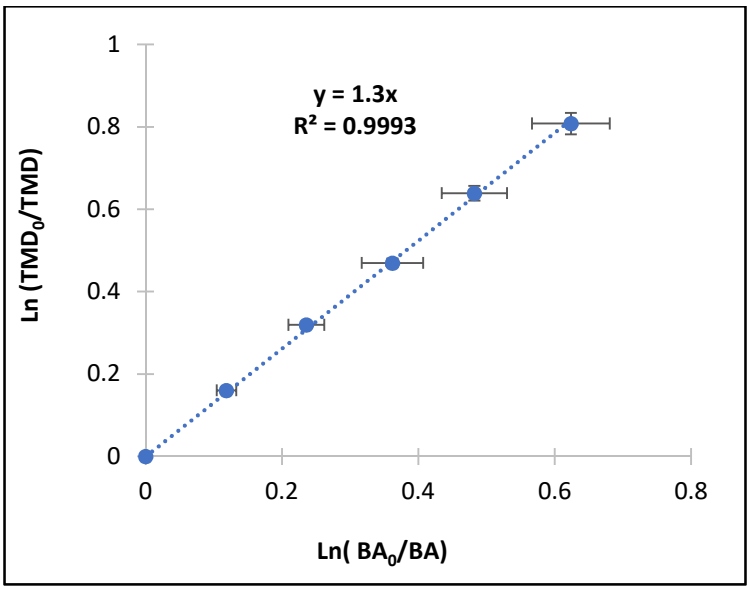

Fig. 3: Determination of absolute (second-order) rate constant of the reaction between TMD and hydroxyl radicals using Eq. 13 under the following experimental conditions: *I* = 50 mA, [Na_2SO_4] = 50 mM, [Fe^{2+}] = 0.1 mM, pH = 3 and room temperature.

3.2 Mineralization of TMD aqueous solution

The total oxidative degradation of the pollutants does not mean that the treated solution is "cleaned" because the formation of intermediate products that can be more toxic (such as the

formation of quinones forms) or persistent than mother molecules. In order to assess an effective treatment, the almost total removal of organics from the solution is required. Therefore the mineralization of 0.1 mM TMD solution was carried out at different current values in terms of TOC removal and results are depicted in Fig. 4. The TOC removal kinetics was very quick; about 99% of organic matter is removed from the solution after 6 h electrolysis for currents above 300 mA demonstrating the efficiency of EF process with BDD anode. Compared to the previously reported works on TRM degradation by advanced oxidation processes, the results obtained in this work show clearly the superiority of electro-Fenton process.

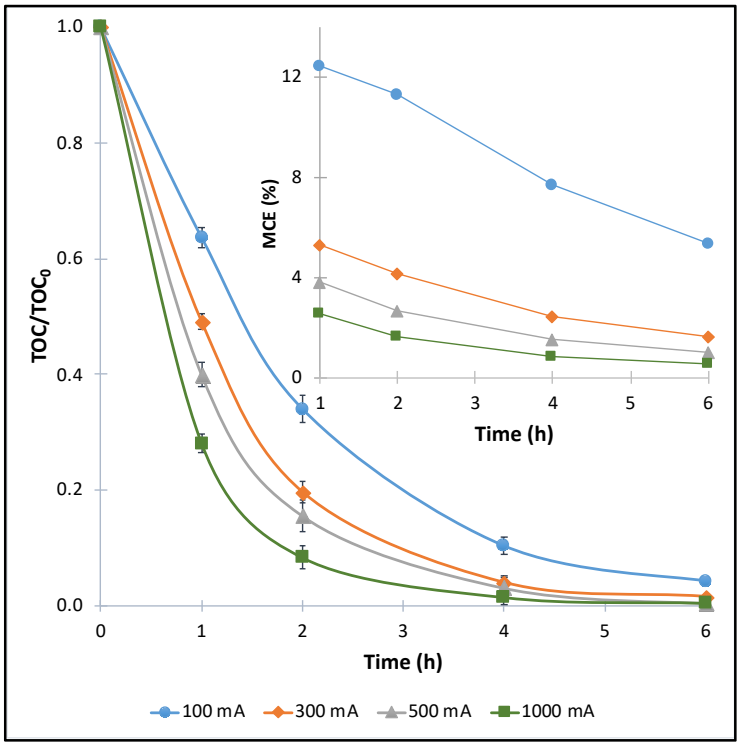

Fig. 4: TOC decay of 0.1 mM TMD solution as a function of current and electrolysis time during EF treatment. Evolution of MCE under same conditions is given in the insert panel. [$NaSO_4$] = 50 mM, [Fe^{2+}] = 0.2 mM, room temperature.

However, as can be seen in Fig. 4, the TOC decay curves are getting closer and closer as the current is increased. The same trend is also highlighted by the MCE curves (inset of Fig. 4)

which represent the proportion of the current used for the mineralization of TMD. After 4 h electrolysis, the MCE was of 7.7, 2.4, 1.5 and 0.86% for 100, 300, 500 and 1000 mA applied currents, respectively. This phenomenon is due to the enhancement of the rate of wasting reactions consuming •OH/M(•OH) (Eqs. 12, 14-16) or electrical energy spent in side reactions (Eqs. 17, 18) producing less powerful oxidation species such as $S_2O_8^{2-}$ and O_3 (Sun and Pignatello, 1993; Brillas et al., 2009; Panizza and Cerisola, 2009; Isarain-Chávez et al., 2010).

$$2\ {}^{\bullet}OH \rightarrow H_2O_2 \quad (14)$$

$$H_2O_2 + {}^{\bullet}OH \rightarrow HO_2^{\bullet} + H_2O \quad (15)$$

$$Fe^{2+} + {}^{\bullet}OH \rightarrow Fe^{3+} + OH^- \quad (16)$$

$$2\ SO_4^{2-} \rightarrow S_2O_8^{2-} + 2\ e^- \quad (17)$$

$$3\ H_2O \rightarrow O_3 + 6\ H^+ + 6\ e^- \quad (18)$$

The EC was also considered to evaluate the cost effectiveness of the process. Figure 5 represents the evolution of EC during the treatment for different currents ranging from 50 to 1000 mA. The results show that higher currents and longer electrolysis time result in high energy consumption, expressed in units of kWh per g TOC removed. This highlights that a compromise between a high efficiency and a low cost have to be encountered. The current value of 300 mA seems to be the best condition as a nearly total mineralization can be reached at a medium cost.

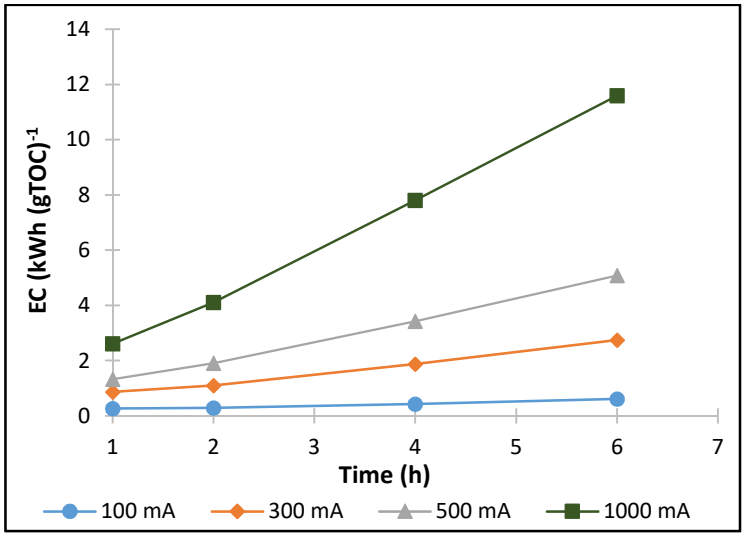

Fig. 5: Evolution of the EC during the electrolysis of 0.1 mM TMD in 50 mM of Na_2SO_4 solution containing 0.2 mM Fe^{2+} as catalyst, under different currents applied.

3.3 Formation and evolution of carboxylic acids and mineral ions

The successive oxidation of organic pollutants by hydroxyl radicals leads to the formation of short-chain carboxylic acids, the ultimate reaction intermediates before complete mineralization step (Brillas et al., 2009). These species are less reactive against hydroxyl radicals and constitute the residual TOC on longer electrolysis times (Oturan et al. 2008; Garcia-Segura and Brillas 2011).

The identification and evolution of three carboxylic acids during EF treatment of TMD were done by ion-exclusion HPLC analysis based on calibration curves prepared from standard compounds (Fig. 6a). The fumaric acid is formed at very low concentration and remained at trace level along electrolysis. The concentration of oxalic acid is lower than that expected compared to previous reports (Dirany et al. 2010; Panizza et al. 2014; Monteil et al. 2019) and completely removed from the solution at 4 h electrolysis. Interestingly, the formation of oxamic acid was not detected. It can be formed at low concentration and quickly mineralized by BDD(•OH). Inversely, fumaric acid is formed in relatively high concentration, reaching

293 0.07 mM at 1 h, before being progressively removed to reach zero concentration value at 6 h
294 electrolysis. The complete mineralization of these carboxylic acids is in agreement with the
295 very low TOC value under the same experimental conditions given in sub-section 3.2.

296

297

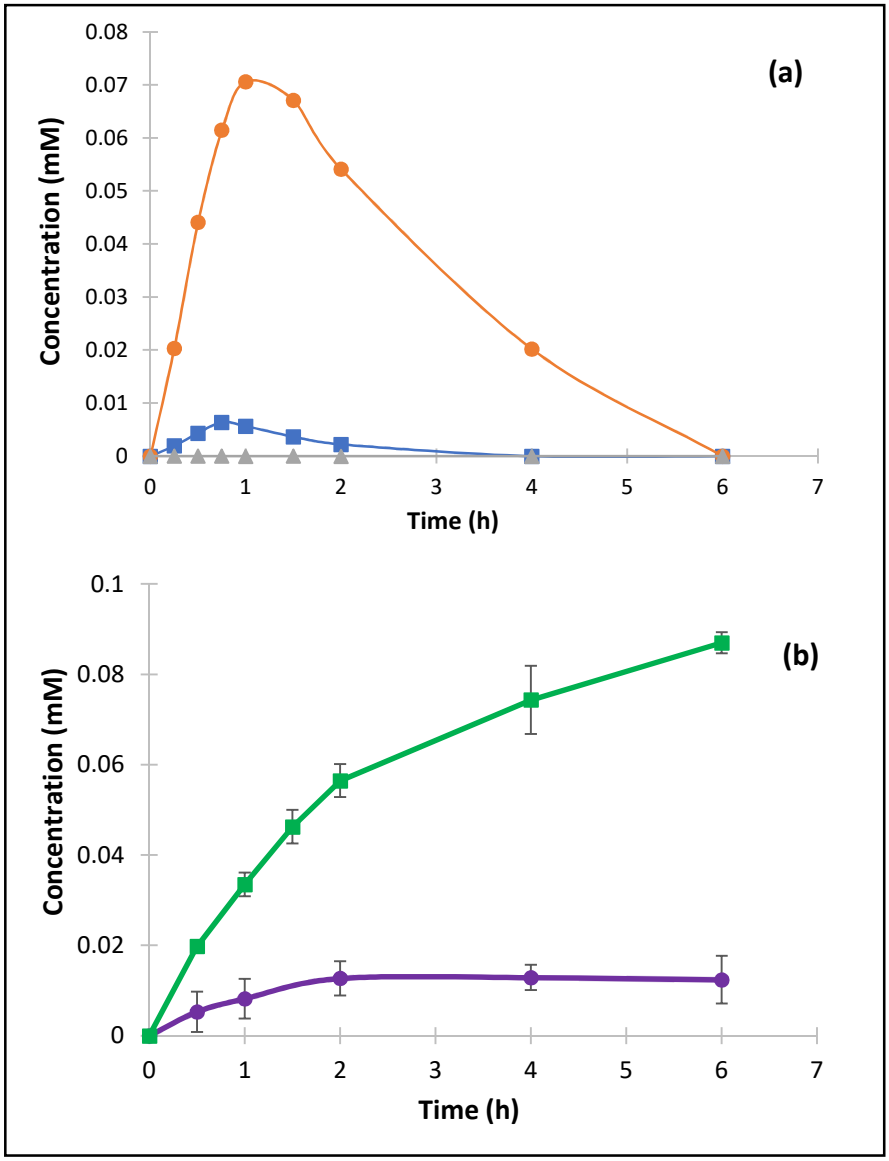

Fig. 6: Evolution of (a) carboxylic acids (oxalic (-■-), glyoxylic (-●-), fumaric (-▲-)) and (b) inorganic ions (NH_4^+ (-■-), NO_3^- (-●-)) during the electrolysis of a 0.1 mM TMD by EF process at 500 mA. The concentration of the supporting electrolyte (Na_2SO_4) was 50 mM for carboxylic acids while it was 15 mM for inorganic ions to avoid the interference of Na^+ ions on analysis of NH_4^+.

Mineral ions formed during the mineralization of 0.1 mM TMD solution were identified and quantified by IC and the results are depicted in Fig. 6b. Ammonium and nitrate ions were formed; however, the amount of ammonium was significantly higher than that of nitrate. The concentration of nitrate remains constant from 2 h electrolysis highlighting its reduction to

ammonium on the large surface carbon felt cathode as reported by several authors (Martin De Vidales et al. 2016; Garcia-Segura et al. 2018). The sum of ammonium and nitrate ions released to the solution was almost the same with the nitrogen (0.1 mM) initially present in TMD molecule.

3.4 Mineralization pathway for TMD solution

The identification of the aromatic oxidation products formed during EF treatment (Table SM-2) as well as the determination of carboxylic acids and inorganic end-products (sub-section 3.3) allowed proposing a plausible degradation pathway of TMD by •OH/M(•OH) generated during EF process (Fig. 7). The intermediates **B** to **G** were identified thanks to the fragmentation analysis of GC-MS spectrum, intermediates **H**, **I** and **J** were identified by ion-exclusion HPLC analysis. Two main routes can be established following paths from **A** to **G** or from **A** to **F**. In the first pathway, an O-demethylation associated with N-demethylations can transform TMD (**A**) into molecule **D**. These reactions were also reported during the degradation of TMD by ferrate and ozone (Zimmermann et al. 2012) and by electrochemical oxidation (Lütke Eversloh et al. 2015). The attack of hydroxyl radicals can also produce a dehydration of TMD producing the intermediate **B** following an O-demethylation. This molecule is then oxidized to product **E** by two N-demethylations. The further attacks of •OH/M(•OH) on the tertiary carbon of molecules **E** and **D** leads to the formation of molecule **G** with releasing ammonium ions (Giannakis et al. 2017; Lambropoulou et al. 2017). The second route starts with the N-demethylation of TMD and the hydroxylation of the aromatic cycle giving molecule **C** which is then followed by an O-demethylation to form intermediate **F**. Finally oxidative ring opening reactions lead to the formation of carboxylic acids **H**, **I** and **J** (Fig. 7).

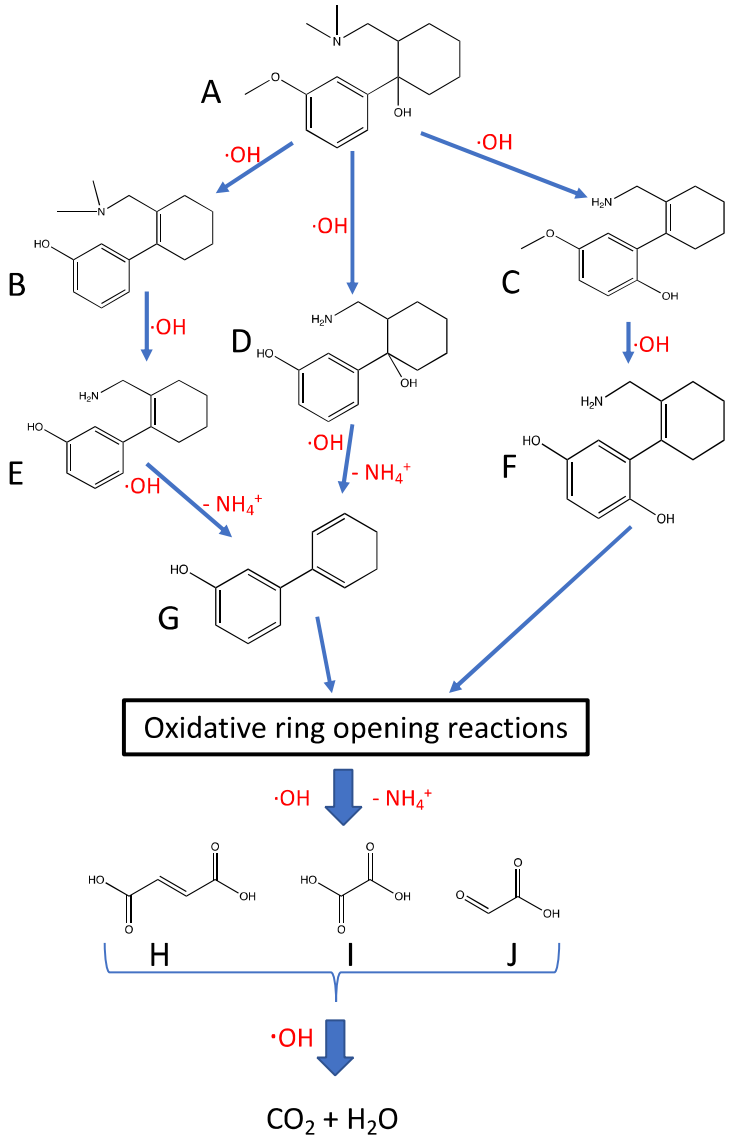

335

336 Fig. 7 n EF

337

338

339 ## 4. Conclusions

340 The degradation of the analgesic TMD in aqueous solutions was assessed, for the first time,
341 by EF process using BDD anode and carbon-felt cathode. It was demonstrated that TMD
342 could be efficiently degraded in 8 min under 500 mA current following a pseudo-first order
343 kinetics. The rate constant of the reaction between TMD and hydroxyl radicals was

344 determined by competition kinetics method and found to be (5.59 ± 0.03) × 10^9 M^{-1} s^{-1}. The
345 complete mineralization of TMD solution was also obtained in 6 h at 500 mA current. This
346 result completed by the analyses of aromatic intermediates and their transformation into
347 carboxylic acids as well as the release of inorganic ions to the solution allowed to proposing a
348 plausible mineralization pathway for oxidative degradation of TMD by hydroxyl radicals. The
349 results obtained in this work showed significantly high degradation kinetics and
350 mineralization efficiency compared to previously reported results for degradation of TRM as
351 can be seen in Table SM-1. Therefore, the electro-Fenton process using BDD anode
352 constitutes a promising alternative to remove efficiently TMD from aqueous medium and can
353 be extended to treatment of other organic pollutants.
354

References:

Antonopoulou M., Hela D., Konstantinou I., 2016. Photocatalytic degradation kinetics, mechanism and ecotoxicity assessment of tramadol metabolites in aqueous TiO2 suspensions. Sci. Total Environ. 545–546, 476–485. doi: 10.1016/j.scitotenv.2015.12.088

Antonopoulou M., Konstantinou I., 2016. Photocatalytic degradation and mineralization of tramadol pharmaceutical in aqueous TiO2 suspensions: evaluation of kinetics, mechanisms and ecotoxicity. Appl. Catal. A: Gen. 515, 136–143. doi: 10.1016/j.apcata.2016.02.005

Brillas E., Sirés I., Oturan M.A., 2009. Electro-fenton process and related electrochemical technologies based on Fenton's reaction chemistry. Chem. Rev. 109, 6570–6631. doi: 10.1021/cr900136g

Buxton G.V., Greenstock C.L., Helman W.P., Ross A.B., 1988. Critical review of rate constants for reactions of hydrated electrons, hydrogen atoms and hydroxyl radicals (•OH/•O-) in aqueous solution. J. Phys. Chem. Ref. Data 17, 513–886. doi: 10.1063/1.555805

Daughton C.G., 2003. Cradle-to-cradle stewardship of drugs for minimizing their environmental disposition while promoting human health. Environ. Health Perspect. 111, 775–785. doi: 10.1289/ehp.5948

Dibyananda M., Samal P.K., Das K., Gouda S.K., Bhoi Y.P., Mishra B.G., 2019. α-NiS/Bi_2O_3 nanocomposites for enhanced photocatalytic degradation of tramadol, ACS Appl. Nano. Mater. 2, 395-407. doi: 10.1021/acsanm.8b01974

Dirany A., Sirés I., Oturan N., Oturan M.A., 2010. Electrochemical abatement of the antibiotic sulfamethoxazole from water. Chemosphere 81, 594–602. doi: 10.1016/j.chemosphere.2010.08.032

Dominguez C.M., Oturan N., Romero A., Santos A., Oturan M.A., 2018. Optimization of electro-Fenton process for effective degradation of organochlorine pesticide lindane. Catal. Today 313, 196–202. doi: https://doi.org/10.1016/j.cattod.2017.10.028

Eversloh C.L., Schulz M., Wagner M., Ternes T.A., 2015. Electrochemical oxidation of tramadol in low-salinity reverse osmosis concentrates using boron-doped diamond anodes. Water Res. 72, 293–304. doi: 10.1016/j.watres.2014.12.021

Ganiyu S.O., Oturan, Trellu C., Raffy S., Cretin M., Causserand C., Oturan M.A., 2019. Electrochemical abatement of analgesic antipyretic 4-aminophenazone using conductive boron-doped diamond and sub-stoichiometric titanium oxide anodes: Kinetics, mineralization and toxicity assessment, ChemElectroChem 6, 1808-1817.

Garcia-Segura S., Brillas E., 2011. Mineralization of the recalcitrant oxalic and oxamic acids by electrochemical advanced oxidation processes using a boron-doped diamond anode. Water Res. 45, 2975–2984. doi: http://dx.doi.org/10.1016/j.watres.2011.03.017

Garcia-Segura S., Lanzarini-Lopes M., Hristovski K., Westerhoff P., 2018. Electrocatalytic reduction of nitrate: fundamentals to full-scale water treatment applications. Appl. Catal. B: Environ. 236,546–568. doi: https://doi.org/10.1016/j.apcatb.2018.05.041

Ghalwa N.A., Abu-Shawish H.M., Zaggout F.R., Saadeh S.M.,Al-Dalou A.R.,Abou Assi A.A. 2014. Electrochemical degradation of tramadol hydrochloride: novel use of potentiometric carbon paste electrodes as a tracer. Arab. J. Chem. 7, 708–714. doi: 10.1016/j.arabjc.2010.12.007

Giannakis S., Hendaoui I., Jovic M., Grandjean D., De Alencastro L.F., Girault H., Pulgarin C., 2017. Solar photo-Fenton and UV / H_2O_2 processes against the antidepressant Venlafaxine in urban wastewaters and human urine . Intermediates formation and biodegradability assessment. Chem. Eng. J. 308, 492–504. doi: 10.1016/j.cej.2016.09.084

Hummel D, Loffler D, Fink G, Ternes TA (2006) Simultaneous determination of psychoactive drugs and their metabolites in aqueous matrices by liquid chromatography mass spectrometry. Environ.

Sci. Technol. 40, 7321–7328.

Isarain-Chávez E., Rodríguez R.M., Garrido J.A., Arias C., Centellas F., Lluís Cabot P., Brillas E., 2010. Degradation of the beta-blocker propranolol by electrochemical advanced oxidation processes based on Fenton's reaction chemistry using a boron-doped diamond anode. Electrochim. Acta 56, 215–221. doi: 10.1016/j.electacta.2010.08.097

Kim I., Yamashita N., Tanaka H., 2009. Performance of UV and UV/H2O2 processes for the removal of pharmaceuticals detected in secondary effluent of a sewage treatment plant in Japan. J. Hazard. Mater. 166, 1134–1140. doi: 10.1016/j.jhazmat.2008.12.020

Kremer ML (2003) The Fenton Reaction. Dependence of the Rate on pH. J. Phys. Chem. A 107, 1734–1741. doi: 10.1021/jp020654p

Lambropoulou D., Evgenidou E., Saliverou V., Kosma C., Constantinou I., 2017. Degradation of venlafaxine using TiO2/UV process: Kinetic studies, RSM optimization, identification of transformation products and toxicity evaluation. J. Hazard. Mater. 323, 513–526. doi: 10.1016/j.jhazmat.2016.04.074

Loos R., Carvalho R., António D.C., Comero S., Locoro G., Tavazzi S., Paracchini B., Ghiani M., Lettieri T., Blaha L., Jarosova B., Voorspoels S., Servaes K., Haglund P., Fick J., Lindberg R.H., Schwesig D., Gawlik B.M., 2013. EU-wide monitoring survey on emerging polar organic contaminants in wastewater treatment plant effluents. Water Res. 47, 6475–6487. doi: 10.1016/j.watres.2013.08.024

Mackul'ak T., Mosny M., Grabic R., Golovko O., Kobab O., Birosová L.,2015. Fenton-like reaction: A possible way to efficiently remove illicit drugs and pharmaceuticals from wastewater. Environ. Toxicol. Pharmacol. 39, 483-488. doi: 10.1016/j.etap.2014.12.016

Martin De Vidales M.J., Millan M., Sáez C., Cañizares P., Rodrigo M.A., 2016. What happens to inorganic nitrogen species during conductive diamond electrochemical oxidation of real wastewater? Electrochem. commun. 67,65–68. doi: 10.1016/j.elecom.2016.03.014

Monteil H., Oturan N., Péchaud Y., Oturan M.A., 2019. Efficient removal of diuretic hydrochlorothiazide from water by electro-Fenton process using BDD anode: a kinetic and degradation pathway study. Environ. Chem. 16, 613-621. doi: 10.1016/j.jece.2019.103400

Monteil H., Péchaud Y., Oturan N., Oturan M.A. 2019. A review on efficiency and cost effectiveness of electro- and bio-electro-Fenton processes: application to the treatment of pharmaceutical pollutants in water. Chem. Eng. J. 376, 119577. doi: https://doi.org/10.1016/j.cej.2018.07.179

Nidheesh P.V., Divyapriya G., Oturan N., Trellu C., Oturan M.A., 2019. Environmental applications of boron-doped diamond electrodes: 1. Applications in water and wastewater treatment. ChemElectrocem 6, 2124–2142. doi: 10.1002/celc.201801876

Nidheesh P.V., Zhou M., Oturan M.A., 2018. An overview on the removal of synthetic dyes from water by electrochemical advanced oxidation processes. Chemosphere 197, 210–227. doi: https://doi.org/10.1016/j.chemosphere.2017.12.195

Oturan M.A., 2000, An ecologically effective water treatment technique using electrochemically generated hydroxyl radicals for in situ destruction of organic pollutants: Application to herbicide 2,4-D. J. Appl. Electrochem. 30, 475–482. doi: 10.1023/A:1003994428571

Oturan M.A., Aaron J.-J., 2014. Advanced oxidation processes in water/wastewater treatment: principles and applications. A Review. Crit. Rev. Environ. Sci. Technol. 44, 2577–2641. doi: 10.1080/10643389.2013.829765

Oturan M.A., Pimentel M., Oturan N., Sirés I., 2008. Reaction sequence for the mineralization of the short-chain carboxylic acids usually formed upon cleavage of aromatics during electrochemical Fenton treatment. Electrochim. Acta 54, 173–182. doi: https://doi.org/10.1016/j.electacta.2008.08.012

Oturan N., Oturan M.A., 2018. Electro-Fenton process : background , new developments and

applications. in: C.A. Martinez-Huitle, M.A. Rodrigo, O. Scialdone (Eds.), Electrochemical Water and Wastewater Treatment, Elsevier, Oxford (UK) and Cambridge (MA-USA), pp. 193-221. https://doi.org/10.1016/B978-0-12-813160-2.00008-0

Oturan N., Zhou M., Oturan M.A., 2010. Metomyl degradation by electro-Fenton and electro-Fenton-like processes: a kinetics study of the effect of the nature and concentration of some transition metal ions as catalyst. J. Phys. Chem. A 114, 10605–10611. doi: 10.1021/jp1062836

Özcan A., Şahin Y., Koparal A.S., Oturan M.A., 2008. Carbon sponge as a new cathode material for the electro-Fenton process: Comparison with carbon felt cathode and application to degradation of synthetic dye basic blue 3 in aqueous medium. J. Electroanal. Chem. 616, 71–78. doi: 10.1016/j.jelechem.2008.01.002

Panizza M., Cerisola G., 2009. Direct and mediated anodic oxidation of organic pollutants. Chem. Rev. 109, 6541–6569. doi: 10.1021/cr9001319

Panizza M., Cerisola G. 2001. Removal of organic pollutants from industrial wastewater by electrogenerated Fenton's reagent. Water Res. 35,3987–3992. doi: 10.1016/S0043-1354(01)00135-X

Panizza M., Dirany A., Sirés I., Haidar H., Oturan N., Oturan M.A., 2014. Complete mineralization of the antibiotic amoxicillin by electro-Fenton with a BDD anode. J. Appl. Electrochem. 44, 1327–1335. doi: 10.1007/s10800-014-0740-9

Park N., Choi Y., Kim D., Kyunghyun K., Junho J., 2018. Prioritization of highly exposable pharmaceuticals via a suspect/non-target screening approach: a case study for Yeongsan river, Korea. Sci. Total Environ. 639, 570–579. doi: 10.1016/j.scitotenv.2018.05.081

Pimentel M., Oturan N., Dezotti M., Oturan M.A., 2008. Phenol degradation by advanced electrochemical oxidation process electro-Fenton using a carbon felt cathode. Appl. Catal. B: Environ. 83, 140–149. doi: 10.1016/j.apcatb.2008.02.011

Rodrigo M.A., Cañizares P., Sánchez-Carretero A., Sáez C., 2010. Use of conductive-diamond electrochemical oxidation for wastewater treatment. Catal. Today 151:173–177. doi: https://doi.org/10.1016/j.cattod.2010.01.058

Rodrigo M.A., Oturan N., Oturan M.A., 2014. Electrochemically assisted remediation of pesticides in soils and water: a review. Chem. Rev. 114, 8720–8745. doi: 10.1021/cr500077e

Rúa-Gómez P.C., Püttmann W., 2013. Degradation of lidocaine, tramadol, venlafaxine and the metabolites O-desmethyltramadol and O-desmethylvenlafaxine in surface waters. Chemosphere 90, 1952–1959. doi: 10.1016/j.chemosphere.2012.10.039

Rúa-Gómez P.C., Püttmann W., 2012. Impact of wastewater treatment plant discharge of lidocaine, tramadol, venlafaxine and their metabolites on the quality of surface waters and groundwater. J. Environ. Monit. 14, 1391–1399. doi: 10.1039/c2em10950f

Sirés I., Brillas E., 2012. Remediation of water pollution caused by pharmaceutical residues based on electrochemical separation and degradation technologies: a review. Environ. Int. 40, 212–229. doi: 10.1016/j.envint.2011.07.012

Sirés I., Brillas E., Oturan M.A., Rodrigo M.A., Panizza M., (2014) Electrochemical advanced oxidation processes: today and tomorrow. A review. Environ. Sci. Pollut. Res. 21, 8336–8367. doi: 10.1007/s11356-014-2783-1

Sirés I., Garrido J.A., Rodríguez R.M., Brillas E., Oturan N., Oturan M.A., 2007. Catalytic behavior of the Fe^{3+}/Fe^{2+} system in the electro-Fenton degradation of the antimicrobial chlorophene. Appl. Catal. B: Environ. 72, 382–394. doi: 10.1016/j.apcatb.2006.11.016

Sopaj F., Oturan N., Pinson J., Podvorica F.I., Oturan M.A., 2016. Effect of the anode materials on the efficiency of the electro-Fenton process for the mineralization of the antibiotic sulfamethazine. Appl. Catal. B: Environ. 199, 331–341. doi: 10.1016/j.apcatb.2016.06.035

Sun Y., Pignatello J.J., 1993. Photochemical reactions involved in the total mineralization of 2,4-D by iron(3+)/hydrogen peroxide/UV. Environ. Sci. Technol. 27, 304–310. doi: 10.1021/es00039a010

Verlicchi P., Galletti A., Petrovic M., Barceló D., Al Aukidy M., Zambello E.,2013. Removal of selected pharmaceuticals from domestic wastewater in an activated sludge system followed by a horizontal subsurface flow bed - analysis of their respective contributions. Sci. Total Environ. 454–455, 411–425. doi: 10.1016/j.scitotenv.2013.03.044

Zhou M., Oturan M.A., Sirès I., 2018. Electro-Fenton process: New trends and scale-up. (ISBN: 978-981-10-6405-0), in: The Handbook of Environmental Chemistry, volume 61, Springer, ISSN: 1867-979X.

Zimmermann S.G., Schmukat A., Schulz M., Benner J., von Gunten U., Ternes T.A.,2012. Kinetic and mechanistic investigations of the oxidation of tramadol by ferrate and ozone. Environ. Sci. Technol. 46:876–884. doi: 10.1021/es203348q